Alcohol Drinking Alters Stress Coping via Extended Amygdala Kappa Opioid Receptor Signaling

Authors: Lara Hwa, Sofia Neira, Meghan Flanigan, Christina Stanhope, Melanie Pina, Dipanwita Pati, Olivia Hon, Waylin Yu, Emily Kokush, Rachel Calloway, Kristen Boyt, Thomas Kash*

Affiliations: Bowles Center for Alcohol Studies, Department of Pharmacology, University of North Carolina at Chapel Hill, 104 Manning Drive, Chapel Hill, NC, 27599, USA

*Correspondence

Thomas L. Kash, Ph.D.

John R. Andrews Distinguished Professor

Bowles Center for Alcohol Studies

Department of Pharmacology

University of North Carolina School of Medicine

Chapel Hill, NC 27599, USA

tkash@email.unc.edu

(919)843-7867

Abstract

BACKGROUND: Maladaptive responses to stress are a hallmark of alcohol use disorder, but the mechanisms that underlie this are not well characterized. OBJECTIVES: Here we show that kappa opioid receptor (KOR) signaling in the bed nucleus of the stria terminalis (BNST) is a critical molecular substrate disrupting stress-coping behavior following heavy alcohol drinking. RESULTS: Altered responses to an innate stressor were associated with enhanced PFC-driven excitation of prodynorphin-containing neurons in the BNST during protracted withdrawal from intermittent alcohol drinking. CONCLUSIONS: These findings suggest that increased corticolimbic connectivity may underlie impaired stress-coping during protracted withdrawal from heavy drinking and represents a target of potential therapeutic mediation as well as a potential biomarker of negative outcomes.

Main Text

Not only do stressors drive both drinking and relapse in alcoholics, but chronic alcohol drinking reciprocally impacts stress systems in the brain. To date, most preclinical research has explored the effects of stressors preceding alcohol drinking (*1*). While blunted responses to stress have been identified in alcohol-dependent individuals (*2*), few studies have considered mechanisms by which alcohol drinking results in maladaptive stress responses during protracted abstinence. This is a critical area of study, as mitigating stress responses can contribute to improved alcohol relapse outcomes. Here, we show that kappa opioid receptor (KOR) dysregulation of corticolimbic circuits underlies lasting behavioral changes to stressors that emerge after chronic drinking.

Male C57BL/6J mice were given six weeks of intermittent access to alcohol (EtOH), a protocol known to induce heavy voluntary drinking (*3*), before behavioral testing both during early (<24 hr) and protracted (7-10 days) abstinence [Fig. 1A, Fig. S1A]. Mice consumed high amounts of EtOH and increased their EtOH preference over time [Fig. 1B]. During early abstinence, we found stress deficits in both the repeated forced swim test (*4*,*5*) [Fig. S1B] and homecage predator odor trimethylthiazoline (TMT) exposure (*6*) [Fig. S1D-G]; however, only responses to the predator odor remain altered throughout protracted abstinence. Specifically, EtOH-drinking mice did not avoid the TMT compared to the water (H_2O)-drinking controls during protracted abstinence [Fig. 1C], suggestive of maladaptive survival behavior. Previous studies have shown that activation of the dynorphin (Pdyn)/KOR system can modulate stress-induced EtOH seeking (*7*), so we tested if KOR blockade could alter drinking-induced stress behavior. Systemic treatment with 5 mg/kg of the long-acting KOR antagonist norBNI rescued the EtOH-induced impairment of predator odor response [Fig. 1D]. Given the potential relevance

of targeting the protracted time point, rather than at acute abstinence [Fig. S1A-G], we next focused on identifying the mechanism for this long-lasting adaptation.

The bed nucleus of the stria terminalis (BNST) is a brain site known for its involvement in stress, anxiety, and addiction, and is regulated by the Pdyn/KOR system (*8*). Initial reports have identified the BNST as a mediator of stress responses to TMT in rats (*9*). We tested whether microinfusions of norBNI directly into the BNST would also alter behavioral responses to TMT during protracted abstinence [Fig. 1G]. Similar to systemic administration, intra-BNST norBNI reduced heightened contact with TMT in the EtOH mice [Fig. 1I-J] with no effect on time spent in the far corners of the home cage [Fig. 1K]. EtOH mice showed significantly less burying behavior in response to TMT compared to H_2O mice, but there was no effect of drug [Fig. 1L].

We then tested if Pdyn neurons in the BNST played a role in this process, as we have previously shown that BNST Pdyn can modulate synaptic transmission in the BNST (*8*). *Pdyn* was deleted from the BNST using the *Pdyn*$^{lox/lox}$ mouse line (*10*) via AAV Cre-GFP microinfusions [Fig. 1M-N]. EtOH mice with BNST Pdyn deletion showed a moderate reduction in TMT contact [Fig. 1O-P] and increased burying behavior compared to control EtOH mice [Fig. 1R]. Importantly, there were no effects of Pdyn deletion in H_2O drinkers. This modest rescue of TMT response in Pdyn deletion EtOH mice may be related to their reduced EtOH consumption compared to GFP controls [Suppl Fig. 1H-K]. These findings demonstrate a role for BNST Pdyn/KOR in regulating specific behavioral responses impaired by long-term EtOH drinking.

Previous studies in rats have shown that TMT increases BNST activity using c-Fos as a marker for active neuronal populations (*11,12*), so we examined this in a line of *Pdyn*-IRES-Cre x Rosa26-flox-stop-L10-GFP (Pdyn-GFP) mice (*13*) after intermittent EtOH or H_2O

consumption [Fig. 2A]. TMT elicited robust dorsal BNST c-Fos immunostaining, which was greater in EtOH mice compared to H_2O mice [Fig. 2C]. Furthermore, TMT increased expression of Pdyn GFP-expressing neurons in the BNST versus non-stressed (NS) mice [Fig. 2D]. Importantly, colocalization of c-Fos in Pdyn-containing cells (BNST^{PDYN}) was largest in the stressed EtOH group [Fig. 2E], suggesting an interaction between EtOH and predator odor stress in the BNST.

To assess dynamic BNST^{PDYN} responses to TMT in real-time, we performed *in-vivo* fiber photometry in EtOH and H_2O mice. Pdyn-Cre mice were injected with a viral construct containing a Cre-inducible genetically-encoded calcium indicator (FLEX-GCaMP7f) and optical fibers were implanted above the BNST [Fig. 2Ff]. When averaged across three TMT exposures, both H_2O and EtOH mice showed sustained increases in BNST^{PDYN} calcium activity in response to TMT [Fig. 2G], which were larger than calcium transients in response to double distilled water (DDW). However, while BNST^{PDYN} responses in H_2O mice did not habituate across trials, EtOH mice displayed reduced BNST^{PDYN} responses in the third TMT trial compared to the first TMT trial [Fig. 2H], suggestive of a blunted stress response. These results indicate that rapid suppression of BNST^{PDYN} activity to stress cues may drive aberrant behavioral responses after chronic drinking.

We next examined the synaptic activity of BNST^{PDYN} neurons following TMT exposure by recording spontaneous excitatory and inhibitory post-synaptic currents (sEPSC, sIPSC) in Pdyn-GFP mice during 7-10 days protracted abstinence [Fig. 2I]. TMT increased sEPSC frequency (Hz) in EtOH and H_2O drinkers compared to non-stressed (NS) mice [Fig. 2J] with no alterations in sIPSC frequency [Fig. 2K]. EtOH and TMT did not impact sEPSC and sIPSC amplitude [Fig. S2A-B]. Increased sEPSC/sIPSC ratios also reflected heightened excitatory drive

onto BNST^{PDYN} cells in stressed mice regardless of drinking history [Fig. 2L]. We were curious if this was an emergent property, similar to incubation of craving, or if this was engaged early in abstinence. To test this, we performed similar experiments and found that during early abstinence, activity of BNST Pdyn neurons is suppressed following alcohol drinking, yet robustly and synergistically engaged following repeated swim exposure in EtOH drinking mice [Fig. S2C-E]. We next sought to examine if KOR played a role in driving this cellular phenotype. Systemic norBNI pretreatment reduced sEPSC frequency in BNST^{PDYN} cells [Fig. 2M-N], but not sIPSC frequency [Fig. 2O], with an increase in the sEPSC/sIPSC ratio being suppressed by norBNI in the EtOH TMT mice [Fig. 2P]. NorBNI did not alter sEPSC or sIPSC amplitude in stressed mice [Fig. S2F-G]. Recordings from non-GFP cells after EtOH and stress [Fig. S2H-K] also revealed heightened sEPSC/sIPSC ratios [Fig. S2J], indicating a general increase in glutamatergic transmission in the BNST. These *ex-vivo* experiments demonstrate that exposure to stress and EtOH induces KOR-mediated alteration of synaptic transmission in the BNST.

To characterize EtOH and stress-specific enhancement of glutamate transmission to the BNST, we labeled inputs to the BNST with the retrograde fluorophore choleratoxin B (CTB) [Fig. S3A] and assessed colocalization with c-Fos following exposure to TMT in EtOH and H_2O mice. Among the known glutamatergic BNST projections, the medial prefrontal cortex (mPFC) showed the largest number of activated inputs, marked by c-Fos and CTB colocalization, in stressed EtOH mice [Fig. S3C; other known projection regions: insula (Fig. S3D) and amygdala (Fig. S3E)]. Since we have previously reported increased glutamatergic transmission in the mPFC following acute TMT exposure (*6*), we wanted to investigate if EtOH and TMT together may strengthen the functional connection between mPFC-BNST.

To investigate the role of mPFC projections to the BNST in alcohol-induced responses to stress, we injected an AAV encoding channelrhodopsin (ChR2) into the mPFC of Pdyn-GFP mice [Fig. 3A] and measured BNST cell responses to photostimulation of this pathway using slice electrophysiology [Fig. S3I-K]. A greater proportion of BNST^{PDYN} neurons were light-responsive after TMT in both H_2O and EtOH mice, whereas non-stressed H_2O mice had mostly non-responsive cells [Fig. 3B]. Similarly, EtOH mice had larger monosynaptic optically-evoked EPSC (oEPSC) amplitudes following TMT compared to H_2O mice and non-stressed EtOH mice [Fig. 3C], with no effects on paired pulse ratio [Fig. 3D]. Both AMPA and NMDA peak amplitudes were greater in BNST^{PDYN} EtOH TMT mice compared to unstressed EtOH mice and H_2O mice [Fig. 3E-F]. There was also an increase in the AMPA/NMDA ratio in the EtOH TMT mice [Fig. 3G], suggesting alcohol drinking may prime the synapse for AMPA receptor recruitment, further contributing to aberrant glutamate signaling and stress reactions. In addition, the EtOH TMT mice were also more resistant to synaptic depression using oEPSC pulse train protocols, suggesting alterations in short-term plasticity [Fig. 3H-K].

Altogether, our findings indicate that engagement of Pdyn/KOR signaling in the BNST promotes an allostatic shift in stress-coping following EtOH drinking. While other studies have found that chronic EtOH exposure and withdrawal can impact glutamatergic function of BNST neurons (*14*), our findings are the first to highlight plastic shifts in response to stressors as well as identifying pathway specific alterations. The engagement of mPFC to BNST is exciting, as a recent study in rats suggested mPFC to BNST signaling governs a response set of coping behavior (*15*). These findings support a role for Pdyn/KORs in the extended amygdala in altering stress coping phenotypes in heavy drinkers. Disentangling this imbalance of stress neuropeptide

signaling may lead to the development of therapeutics to enhance stress coping in persons with alcohol use disorder.

References:

1. N. W. Gilpin, J. L. Weiner, Neurobiology of comorbid post- traumatic stress disorder and alcohol- use disorder. *Genes, Brain and Behavior* **16**, 15-43 (2017).
2. R. Sinha *et al.* Effects of adrenal sensitivity, stress-and cue-induced craving, and anxiety on subsequent alcohol relapse and treatment outcomes. *Arch Gen Psychiatry* **68**, 942-952 (2011).
3. L.S. Hwa *et al.* Persistent escalation of alcohol drinking in C57BL/6J mice with intermittent access to 20% ethanol. *Alcohol. Clin. Exp. Res.* **35**, 1938-1947 (2011).
4. R. I. Anderson *et al*. Forced swim stress increases ethanol consumption in C57BL/6J mice with a history of chronic intermittent ethanol exposure. *Psychopharmacology* **233**, 2035-2043 (2016).
5. K. G. Commons *et al*. The rodent forced swim test measures stress-coping strategy, not depression-like behavior. *ACS. Chem. Neurosci.* **8**, 955-960 (2017).
6. L. S. Hwa *et al*. Predator odor increases avoidance and glutamatergic synaptic transmission in the prelimbic cortex via corticotropin-releasing factor receptor 1 signaling. *Neuropsychopharmacology* **44**, 766-775 (2019).
7. A. D. Lê *et al*. Role of κ-opioid receptors in the bed nucleus of stria terminalis in reinstatement of alcohol seeking. *Neuropsychopharmacology* **43**, 838-850 (2018).
8. N. A. Crowley *et al*. Dynorphin controls the gain of an amygdalar anxiety circuit. *Cell reports* **14**, 2774-2783 (2016).
9. M. Fendt *et al*. Temporary inactivation of the bed nucleus of the stria terminalis but not of the amygdala blocks freezing induced by trimethylthiazoline, a component of fox feces. *J. Neurosci.* **23**, 23-28 (2003).

10. D. Bloodgood *et al.* https://www.biorxiv.org/content/10.1101/663666v1.abstract (2019).

11. H. E. Day *et al.* The pattern of brain c-fos mRNA induced by a component of fox odor, 2, 5-dihydro-2, 4, 5-trimethylthiazoline (TMT), in rats, suggests both systemic and processive stress characteristics. *Brain Res.* **1025**, 139-151 (2004).

12. A. Asok *et al*. Immediate early gene and neuropeptide expression following exposure to the predator odor 2, 5-dihydro-2, 4, 5-trimethylthiazoline (TMT). *Behav. Brain Res.* **248**, 85-93 (2013).

13. R. Al-Hasani *et al*. Distinct subpopulations of nucleus accumbens dynorphin neurons drive aversion and reward. *Neuron* **87**, 1063-1077 (2015).

14. Z. A. McElligott, D. G. Winder. Modulation of glutamatergic synaptic transmission in the bed nucleus of the stria terminalis. *Prog. Neuropsychopharmaco.l Biol. Psychiatry*. **33**, 1329-1335 (2009).

15. S. B. Johnson *et al.* Prefrontal–bed nucleus circuit modulation of a passive coping response set. *J. Neurosci*. **39**, 1404-1419 (2019).

Materials and Methods:

Animals. Eight-week old male C57BL/6J mice (Jackson Laboratories, Bar Harbor, ME) were used for behavioral pharmacology experiments. To visualize Pdyn-expressing neurons, we generated a Pdyn-GFP reporter line by crossing *preprodynorphin*-IRES-Cre mice (*8,10,13*) (Pdyn-Cre) and Rosa26-flox-stop-L10-GFP reporter mice. For conditional knockout of BNST Pdyn, we used the *Pdyn*$^{lox/lox}$ mouse line (*10*). These mice were bred in the UNC facilities. All mice were group-housed for at least 3 days before being singly housed in polycarbonate cages (GM500, Tecniplast, Italy) with a 12:12-h reversed dark-light cycle with lights off at 7:00am. Mice had unrestricted access to food (Prolab Isopro RMH 3000, LabDiet, St. Louis, MO) and H_2O. The UNC School of Medicine Institutional Animal Care and Use Committee approved all experiments. Procedures were conducted in accordance with the NIH Guidelines for the Care and Use of Laboratory Animals.

Intermittent EtOH Drinking. Mice were given 24 hr access to a 20% (w/v) EtOH solution and water on an intermittent schedule (*3*). Two bottles were held in modified drinking spouts of plastic cage tops and weighed before and after daily EtOH access. A dummy cage without an animal was used to simulate fluid lost while positioning the bottles, so average fluid drip was subtracted from each mouse's daily drinking. Mice were tested for stress reactions to TMT during 7-10 day protracted abstinence after 6 weeks of intermittent drinking. Separate groups of mice were tested for stress reactions to forced swim and TMT predator odor after 8 weeks of intermittent drinking.

Behavioral Assays after EtOH Drinking

Repeated Forced Swim Test. Mice were placed into an acrylic cylinder filled with 23-25° water 4 hr before access to EtOH for 10 min (*4*). Immobility duration was hand-scored by a blind

observer across two trials. Increases in immobility time across forced swim trials were interpreted as an adaptive stress coping strategy (*5*).

TMT Predator Odor Exposure. Exposure to fox-derived synthetic predator odor, trimethylthiazoline (TMT), was performed in the home cage as previously described to elicit stress reactions in mice (*6*). For a baseline pre-trial period, mice habituated to a cotton tip applicator held vertically in place for 10 min in the home cage. The TMT trial occurred when 2.5 µl TMT was applied to the cotton tip followed by 10 min of behavioral observation. Duration of contact with the TMT object, time spent in the far corners of the cage, and distance traveled (sec) were recorded and quantified with Ethovision XT13 (Noldus, The Netherlands), and burying was hand-scored using BORIS (Behavioral Observation Research Interactive Software) by a blind observer. Heatmaps were generated through Ethovision XT13.

Stereotaxic Surgery. Adult mice (>8 weeks) were deeply anesthetized with 3-4% isoflurane in oxygen and placed into a stereotaxic frame (Kopf Instruments, Tujunga, CA) while on a heated pad. Isoflurane anesthesia was maintained at 1-2% during the remainder of the surgery. After sterilization with 70% ethanol and betadine, a scalp incision was made and burr holes were drilled above the target. A 1 µl Neuros Hamilton syringe (Hamilton, Reno, NV) microinjected the virus or drug at a rate of 0.1 µl/min. Coordinates for the BNST were AP +0.30 mm, ML +/- 0.95 mm, DV -4.35 mm from bregma. Coordinates for the mPFC were AP +1.70 mm, ML +/- 0.30 mm, DV -2.50 mm from bregma. For fiber photometry surgery, both virus and 4.5 mm ceramic ferrules (Neurophotometrics Ltd, CA) were implanted at a 10° angle. Mice recovered for one week before testing.

Drugs and Viral Vectors. 5 mg/kg norBNI (Cat no. 0347, Tocris) was administered i.p., 1ml/100g, 16 hr before testing to both EtOH and H_2O mice. For intra-BNST norBNI

microinfusions, 5 ug/ul norBNI was injected with 50 nl AAV5-CamKII-eGFP to mark the injection site. *Pdyn*$^{lox/lox}$ mice received 300 nl AAV5-CamKII-Cre-eGFP (UNC Vector Core, Lot 6450) and control AAV5-CamKII-eGFP (Lot 4621B) in the BNST. Fiber photometry experiments used 300 nl AAV9-syn-FLEX-GCaMP7f and ceramic ferrules in Pdyn-Cre mice. Choleratoxin B (CTB) 555 (Invitrogen) was used for retrograde tracing injected 7 days before testing. 300 nl AAV5-CamKIIa-hChR2(H134R)-mCherry-WPRE-hGH (Addgene, Lot CS1096) was injected into the mPFC of Pdyn-GFP mice for synaptic connectivity experiments in the BNST. All intracranial injections were bilateral.

c-Fos Immunohistochemistry, Histology, and Microscopy. Mice were deeply anesthetized with Avertin before transcardial perfusion with phosphate buffered saline and 4% paraformaldehyde. Brains were extracted, cryoprotected, and then sliced on a Leica 1200S vibratome. Coronal sections of the Pdyn-GFP mice were stained for *c-Fos* immunofluorescence to visualize colocalization of Pdyn-containing (GFP) and *c-Fos* expressing cells. In separate mice, the retrograde fluorescent tracer choleratoxin B (CTB) 555 was injected into the BNST of C57BL/6J mice. The immunofluorescence protocol for *c-Fos* was performed according to previous studies (*6*) using tyramine signal amplification (TSA). After PBS washes, 50% methanol, and 3% hydrogen peroxide, tissue was incubated in blocking buffer with 0.3% Triton X-100 and 1% bovine serum albumin for 60 min. Slices were then incubated at 4°C for 48 hr in blocking buffer containing a rabbit anti-*c-Fos* antibody (1:3000, ABE457, Millipore, Bellerica, MA). After washes in TNT (0.1 M Tris-HCl, 0.15 M NaCl, 3% TritonX-100) and TNB (0.1 M Tris-HCl, 0.15 M NaCl, 0.5% Perkin Elmer blocking reagent) buffer, slices were incubated in a goat anti-rabbit horse radish peroxidase-conjugated IgG (1:200, NEF812001EA, PerkinElmer, Waltham, MA) for 30 min. After TNT washes, tissue was processed using a TSA kit with Cy3-tyramide

(1:50, PerkinElmer, Waltham, MA) for 10 min. For placement verification, viral injection sites were verified using a wide-field epifluorescent microscope (BX-43, Olympus, Waltham, MA). For quantification of *c-Fos* immunofluorescence and CTB tracing, slices were imaged on a Zeiss 800 laser scanning confocal microscope (Carl Zeiss, Germany) and analyzed with Zeiss Zen 2 Blue Edition software.

Fiber photometry

Apparatus. A branched fiber optic patch cord (Doric Lenses, BFP_200/230/900-0.37_FC-MF1.25) connected to the fiber photometry apparatus (Neurophotometrics, Ltd.) was attached bilaterally to implanted fiber optic cannulae using cubic zirconia sleeves. To record fluorescence signals from GCaMP7f, light from a 470 nm LED was bandpass filtered, collimated, reflected by dichroic mirrors, and focused by a 20x objective. LED light was delivered at a power that resulted in 35-50 µW of 470 nm light at the tip of the patch cord. Emitted GCaMP7f fluorescence was bandpass filtered and focused on the sensor of a CCD camera. The end of the fiber was imaged at a rate of 40 frames per sec, and the mean value of a ROI of a cross-section of the fiber was calculated using the open-source software Bonsai. To serve as an isosbestic control channel, 415 nm LED light was delivered sequentially with 470 nm LED light in a similar manner. Recording data were aligned with behavior using keystroke timestamps for behavioral video capture start.

Analysis. Analysis of fiber photometry signals was performed using custom-written MATLAB code (Mathworks, Inc.). GCaMP7f (470 nm) and isosbestic (415 nm) signals were de-interleaved, low-pass filtered (2 Hz), fit with a biexponential curve that was then subtracted from filtered data to correct for bleaching, and normalized by calculating the change from mean

fluorescence (ΔF/F) and z-scoring. Odor-associated GCaMP7f activity was determined by calculating the AUC of transients aligned to the completion of odor delivery.

Behavior. To record from BNST^{PDYN} neurons in response to TMT, Pdyn-Cre mice were injected with AAV-FLEX-GCaMP7f and ferrules were implanted above the BNST. Mice were habituated to patch cords for three days before odor testing. On the day of odor testing, mice were exposed to three sequential trials each of double distilled water (DDW) and the predator odor TMT in the home cage. Two min of baseline recordings were collected before odor delivery and recording continued for 5 min following odor delivery. To minimize the role of the experimenter during testing, the odors were delivered via syringe pump attached to polyethylene tubing. The liquid odors were contained between air bubbles and DDW to prevent odor leak prior to intended delivery.

Slice Electrophysiology. Ninety minutes following TMT, which was also 24 hr after the last EtOH access, mice were sacrificed via deep isoflurane anesthesia, and coronal brain slices containing the BNST were collected according to standard laboratory protocols (*6,8,10*). Whole-cell voltage-clamp electrophysiological recordings were performed in BNST^{PDYN} cells visualized using a 470 nm LED. The effects of EtOH and TMT on basal synaptic transmission were assessed in voltage clamp by adjusting the membrane potential and using a cesium methanesulfonate-based intracellular solution (135 mM cesium methanesulfonate, 10 mM KCl, 10mM HEPES, 1 mM MgCl2, 0.2 mM EGTA, 4 mM MgATP, 0.3 mM GTP, 20 mM phosphocreatine, pH 7.3, 285-290 mOsmol). Lidocaine n-ethyl bromide (1 mg/ml) was included in the intracellular solution to block postsynaptic sodium currents. Neurons were held at -55 mV to assess glutamatergic synaptic transmission. In the same cell, neurons were held at +10 mV to assess GABAergic synaptic transmission. Fluctuations in current were used to determine

spontaneous post-synaptic current (sEPSC or sIPSC) frequency and amplitude, as well as to calculate sEPSC/sIPSC ratios. Synaptic transmission experiments in BNST^{PDYN} cells were also performed in animals that received 5 mg/kg norBNI i.p. 16 hr prior to TMT. Electrophysiological recordings were then analyzed using Clampfit 10.7 software (Molecular Devices, Sunnyvale, CA).

For *ex-vivo* optogenetic experiments, tissue was evaluated for light-evoked action potentials in the mPFC. Brains were discarded and not used for further experimentation if injection sites were missed or if action potentials were not present. A blue LED (470 nm, CoolLed) was used to optically stimulate release from channelrhodopsin (ChR2)-containing fibers (*8*). Picrotoxin (25 uM), tetrodotoxin (500 nM), and 4-AP (200 uM) were added to the aCSF to isolate monosynaptic oEPSCs with cells held at -70 mV. The intracellular solution was cesium gluconate (117 mM D-gluconic acid and cesium hydroxide, 20 mM HEPES, 0.4 mM EGTA, 5 mM tetraethyl ammonium chloride, 2 mM MgCl26H2O, 4 mM Na2ATP, 0.4 Na2GTP, pH 7.3, 287-292 mOsmol). oEPSC amplitude (pA) was the first peak of the paired pulse ratio with a 50 ms interstimulus interval. Paired pulse ratio was calculated as the second peak amplitude divided by the first peak amplitude. Cells were held at -70 mV to isolate AMPAR-mediated current and at +40 mV for NMDAR-mediated current. In separate slices, ten 1, 5, and 10 Hz pulse trains were performed at -55 mV voltage clamp without the presence of ionotropic inhibitors with the cesium methanesulfonate internal solution. The nine subsequent amplitudes in the pulse train were normalized to the first peak.

Statistics. Time spent in contact with the TMT, far corners, and burying behavior in sec were analyzed with two-way ANOVA with drug/virus and EtOH as factors. Post-hoc paired and unpaired t-tests were two-tailed and used where appropriate as described in Figure Legends. In

experiments where virus was injected before EtOH, cumulative 6-week alcohol intake and average ethanol preference were compared via t-test. BNST *c-Fos*, Pdyn-containing, and *c-Fos* and Pdyn colocalization were analyzed with two-way ANOVA with TMT exposure and EtOH as factors. Fiber photometry ΔF/F calcium signals were transformed into z-scores and area under the curve. Responses between TMT trial 1 and trial 3 were compared with a paired t-test. Synaptic transmission measures (e.g. sEPSC frequency) were analyzed with two-way ANOVA with TMT exposure and EtOH as factors. With norBNI physiology, only stressed mice with no injection were compared with norBNI-injected stressed mice in separate two-way ANOVA with drug and EtOH as factors. To compare proportion of light-responsive cells per condition, a X^2 test was performed. Furthermore, optically-evoked experiments (e.g. oEPSC amplitude) were analyzed with two-way ANOVAs comparing TMT and EtOH exposure. Pulse trains were analyzed with repeated measures two-way ANOVA across stimulus time and condition. Alpha was set to 0.05. Statistical tests were analyzed with GraphPad Prism 8 (La Jolla, CA, USA).

Acknowledgments

Funding: This work was supported by the National Institutes of Health [grant numbers K99AA027576 (LSH), T32AA007573 (MEF), F32AA026485 (MMP), F31AA027129 (WY), R01AA019454 (TLK), U01AA020911 (TLK), and R01AA025582 (TLK)]. **Author Contributions:** LSH, SN, CS, EK, and RC performed and analyzed behavioral tests. LSH, MEF, and OH provided support for and analyzed the fiber photometry experiments. LSH, SN, MMP, and DP assisted with electrophysiology experiments. WY and KB provided additional technical expertise. LSH and TLK conceptualized, designed the study, and wrote the manuscript.

Competing Interests: Authors declare no competing interests. **Data and materials availability:** All data are available in the main text or the supplementary materials.

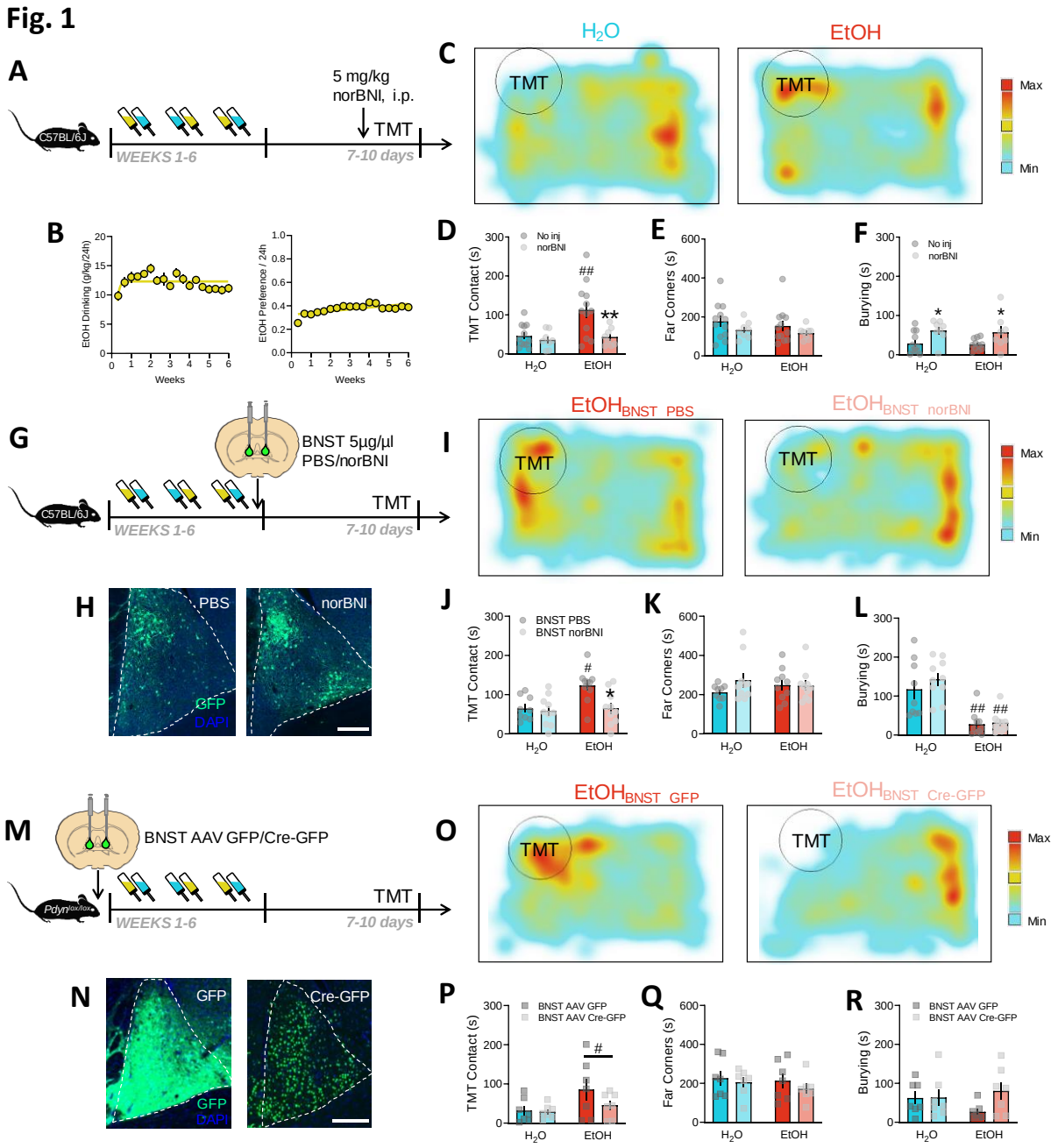

Fig. 1. BNST KOR regulation of responses to TMT predator odor after long-term alcohol drinking. **A**, Experimental protocol for 5 mg/kg i.p. KOR antagonist manipulation of predator odor behavior after intermittent EtOH. **B**, EtOH drinking (g/kg/24hr) and preference / 24hr of male C57BL/6J mice included in a-f and g-l (n=24 mice). **C**, Representative heatmaps of individual H_2O (left) and EtOH (right) spatial location. The circle indicates TMT location. Red color indicates maximum time spent. Aqua color indicates minimum time spent. Pretreatment with norBNI affected: **D**, TMT contact (sec): interaction $F_{1,36}$=4.47, p=0.042; no injection H_2O vs EtOH t_{36}=3.75, ##p=0.0027; EtOH no injection vs norBNI t_{36}=3.48, **p=0.0012. **E**, Time spent in the far corners (sec), and **F**, Burying (sec): norBNI main effect $F_{1,36}$=12.08, p=0.0014;

H_2O no injection vs norBNI t_{35}=2.56, *p=0.0299; EtOH no injection vs norBNI t_{35}=2.36, *p=0.0472. **G**, Experimental design for 5 µg/µl norBNI in the BNST. **H**, Representative images of BNST infusions of PBS (n=9 H_2O, n=10 EtOH) and norBNI (n=10 H_2O, n=10 EtOH) marked with GFP. Scale bar indicates 200 µM. **I**, Representative heatmaps of TMT-induced activity with EtOH BNST PBS (left) and EtOH BNST norBNI (right). **J**, TMT contact (sec): interaction $F_{1,35}$=4.30, p=0.0454; PBS H_2O vs EtOH t_{35}=3.29, #p=0.0105; EtOH PBS vs norBNI t_{35}=3.32, *p=0.0105. **K**, Far Corners (sec). **L**, Burying (sec): EtOH main effect $F_{1,35}$=42.65, p<0.001; PBS H_2O vs EtOH t_{35}=4.06, ##p=0.0010; norBNI H_2O vs EtOH t_{35}=5.19, ##p<0.001. **M**, Time course of deletion of BNST Pdyn in *Pdyn*$^{lox/lox}$ mice before EtOH and TMT. **N**, Images of AAV-GFP and AAV-Cre-GFP expression (H_2O GFP n=7, Cre-GFP n=7. EtOH GFP n=7, Cre-GFP n=7). Scale bar measures 200 µM. **O**, Sample TMT heatmaps of EtOH BNST GFP (left) and EtOH BNST Cre-GFP (right) mice. **P**, TMT contact (sec): EtOH main effect $F_{1,24}$=4.65, #p=0.0114. **Q**, Far Corners (sec). **R**, Burying (sec). EtOH GFP vs EtOH Cre-GFP t_{12}=2.28, p=0.0415.

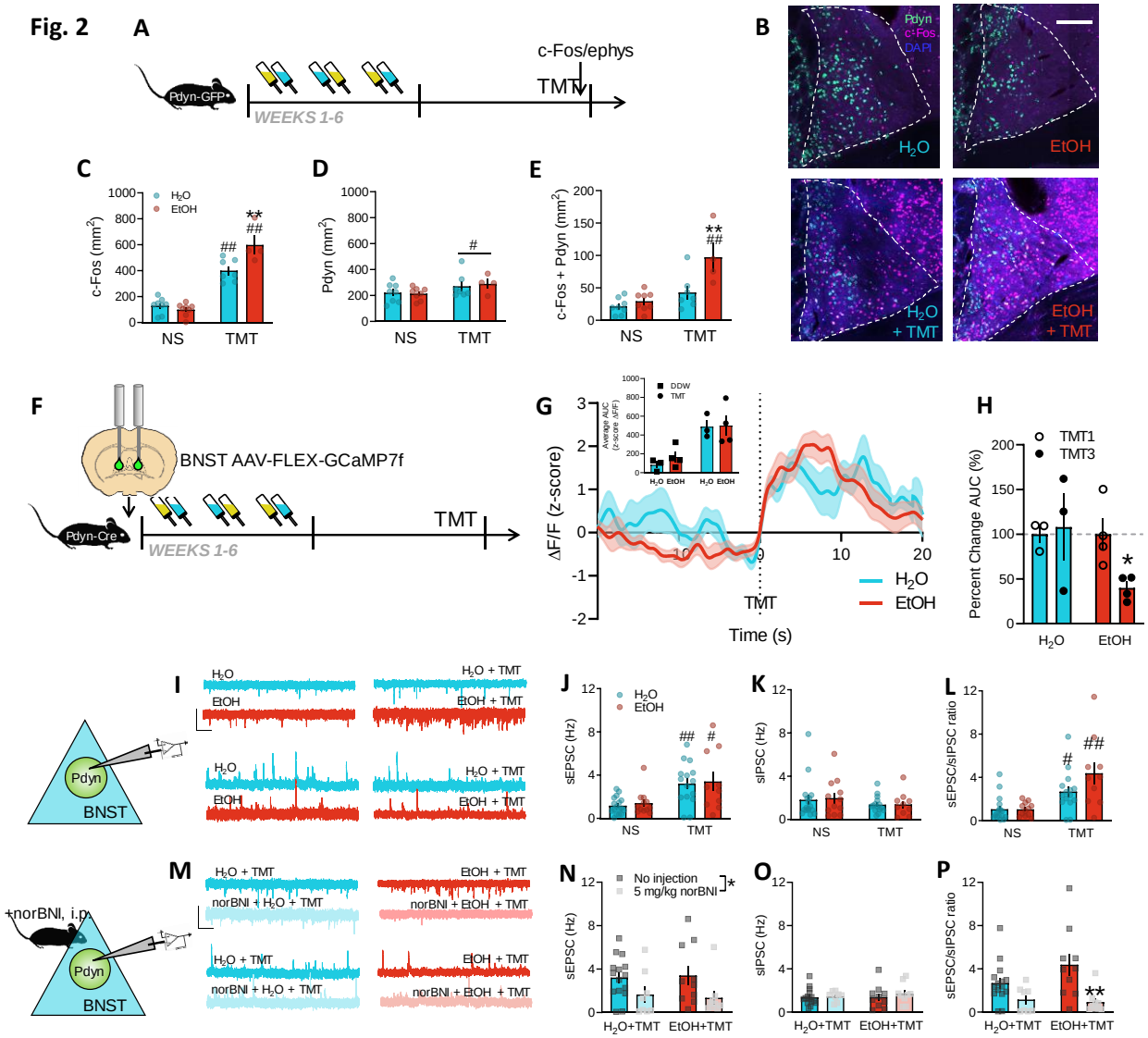

Fig. 2. BNST as a critical site for prodynorphin neurons activated after stress during protracted withdrawal from alcohol. **A**, Schematic of obtaining BNST tissue for c-Fos immunohistochemistry or recording electrophysiology after EtOH and TMT in Pdyn-GFP mice. **B**, Representative images of Pdyn (green) and c-Fos Cy3 immunostaining (pseudocolored purple) in H_2O (n=8), EtOH (n=8), H_2O + TMT (n=7), and EtOH + TMT (n=4) conditions. Scale bar is 200 µm. **C**, BNST c-Fos quantification (mm^2): interaction $F_{1,23}$=12.45, p=0.0018; H_2O non-stress (NS) vs TMT t_{23}=6.51, ##p<0.0001; EtOH NS vs TMT t_{23}=10.13, ##p<0.0001; TMT H_2O vs TMT EtOH t_{23}=3.92, **p=0.0041. Aqua bars are H_2O, red bars are EtOH. **D**, Pdyn-GFP quantification (mm^2): TMT main effect $F_{1,23}$=4.56, #p=0.0437. **E**, Colocalization between c-Fos and Pdyn-GFP (mm^2): interaction $F_{1,23}$=5.91, p=0.0233; EtOH NS vs TMT t_{23}=4.66, ##p=0.0007; TMT H_2O vs TMT EtOH t_{23}=3.65, **p=0.0081. **F**, Fiber photometry experimental design with Cre-inducible GCaMP7f in the BNST of Pdyn-Cre mice (n=3 H_2O, n=4 EtOH). **G**, BNST^{PDYN} calcium transients (z-scores of Δf/f) after H_2O (aqua) and TMT (red) with inset average area under the curve (AUC) after DDW (squares) and TMT (circles). **H**, Percent change in AUC across 3 TMT exposures. EtOH TMT 1 vs TMT 3 t_3=3.35 *p=0.0441. **I**, Representative

traces of BNST^{PDYN} cell synaptic transmission in H_2O (n=6, 17 cells), EtOH (n=4, 12 cells), H_2O + TMT (n=5, 15 cells), and EtOH + TMT (n=4, 10 cells). Scale bar indicates 50 pA height and 1 sec time. **J**, Spontaneous excitatory post-synaptic currents (sEPSC) frequency (Hz): TMT main effect $F_{1,50}$=18.24, ##p<0.0001; H_2O NS vs TMT t_{50}=3.38, p=0.0028; EtOH NS vs TMT t_{50}=2.75, p=0.0167. **K**, Spontaneous inhibitory post-synaptic currents (sIPSC) frequency (Hz). **L**, sEPSC/sIPSC ratio: TMT main effect $F_{1,50}$=23.61, p<0.0001; H_2O NS vs TMT t_{50}=2.50, p=0.0312; EtOH NS vs TMT t_{50}=4.24, p=0.0002; TMT H_2O vs EtOH t_{50}=2.25, p=0.0566. **M**, Sample traces of BNST^{PDYN} cell synaptic transmission after 16 hr pretreatment with 5 mg/kg norBNI, i.p. Light aqua is norBNI + H_2O + TMT (n=3, 8 cells). Light red is norBNI + EtOH + TMT (n=3, 9 cells). Scale bar equals 50 pA height and 1 sec time. The non-injected H_2O + TMT and EtOH + TMT cells were used from panels j-l. **N**, sEPSC frequency (Hz): norBNI main effect $F_{1,38}$=6.96, *p=0.0120. **O**, sIPSC frequency (Hz). **P**, sEPSC/sIPSC ratio: norBNI main effect $F_{1,38}$=14.42, p=0.005; EtOH + TMT non-injected vs norBNI t_{38}=3.63, **p=0.0017.

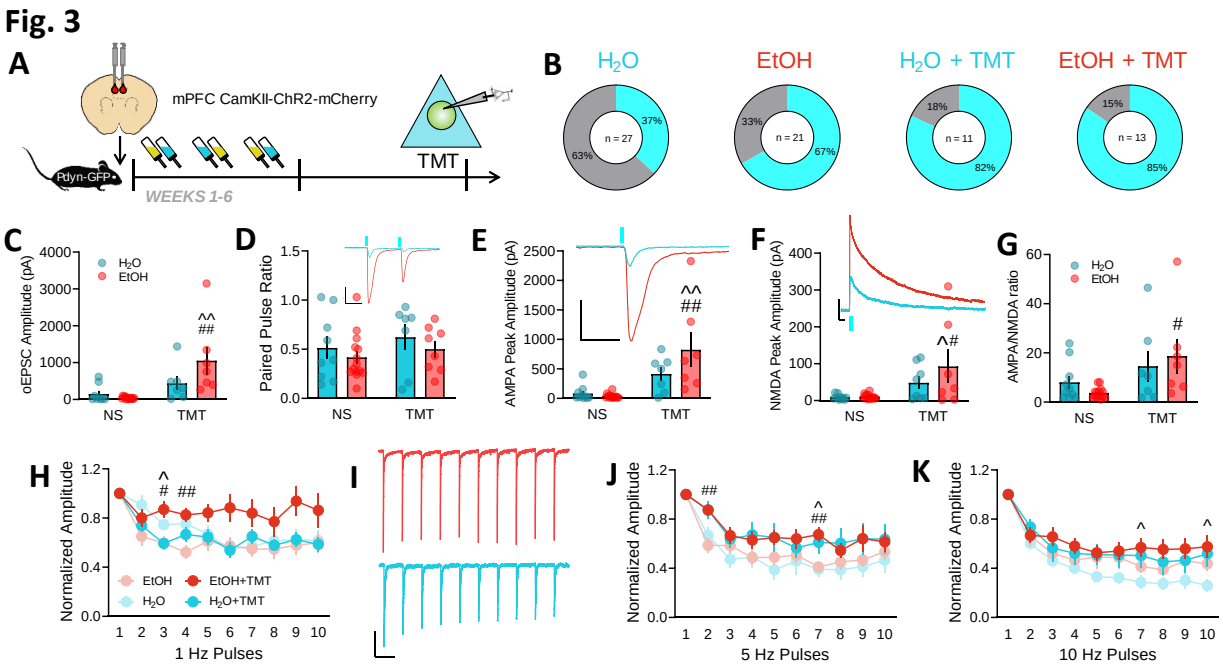

Fig. 3. Cortical input onto BNST^{PDYN} cells gates stress-enhanced glutamatergic plasticity after history of alcohol. **A**, Experimental design testing synaptic connectivity of mPFC input to BNST^{PDYN} cells using channelrhodopsin (ChR2) after EtOH and TMT. **B**, Proportions of light-responsive (aqua) and non-light-responsive (grey) BNST^{PDYN} cells to optically-evoked EPSC in H_2O (10/27 responsive cells, n=7), EtOH (14/21 responsive cells, n=5), H_2O + TMT (9/11 responsive cells, n=4), and EtOH + TMT (11/13 responsive cells, n=4) groups: X^2_3=21.43, **p<0.0001. **C**, mPFC-BNST^{PDYN} oEPSC amplitude (pA): interaction $F_{1,33}$=4.74, *p=0.0367; H_2O non-stress (NS) vs EtOH + TMT t_{33}=3.70 ^^p=0.0047; EtOH NS vs EtOH + TMT t_{33}=4.50, ##p=0.0005. **D**, Paired pulse ratio. Inset example traces of H_2O + TMT (aqua) and EtOH + TMT (red) with blue LED onset. Scale bar indicates 200 pA height and 50 ms time. **E**, AMPA peak amplitude (pA): TMT main effect $F_{1,34}$=22.03, p<0.0001; H_2O NS vs EtOH + TMT t_{34}=4.28, ^^p=0.0009; EtOH NS vs EtOH + TMT t_{34}=4.82, ##p=0.0002. Inset AMPA traces of H_2O + TMT (aqua) and EtOH + TMT (red) with blue LED onset. Scale bar indicates 200 pA height and 50 ms time. **F**, NMDA peak amplitude (pA): TMT main effect $F_{1,34}$=12.09, p=0.0148; H_2O NS vs EtOH + TMT t_{34}=3.13, ^p=0.0213; EtOH NS vs EtOH + TMT t_{34}=3.27, #p=0.0148. Inset NMDA traces of H_2O +TMT (aqua) and IA+TMT (red) with blue LED onset. Scale bar indicates 200 pA height and 50 ms time. **G**, AMPA/NMDA ratio: TMT main effect $F_{1,34}$=8.12, p=0.0074; EtOH NS vs EtOH + TMT t_{34}=2.89, #p=0.0132. **H**, oEPSC normalized amplitude across 1 Hz pulse trains: interaction $F_{27,351}$=1.83, p=0.0080; Pulse 3: EtOH NS vs EtOH + TMT $t_{22.81}$=3.21, #p=0.0234; H_2O + TMT vs EtOH + TMT $t_{18.81}$=3.40, ^p=0.0180; Pulse 4: EtOH NS vs EtOH + TMT $t_{23.99}$=3.95, ##p=0.0036. **I**, Representative traces of 1 Hz pulse trains in EtOH + TMT (red) and H_2O + TMT (aqua) BNST^{PDYN} cells. Scale bar indicates 200 pA height and 1 sec time. **J**, oEPSC normalized amplitude across 5 Hz pulse trains: pulse main effect $F_{9,351}$=45.58, p<0.000; Pulse 2: EtOH NS vs EtOH + TMT $t_{23.22}$=3.84, ##p=0.0049; Pulse 7: H_2O vs EtOH + TMT $t_{19.76}$=3.52, ^p=0.0131; EtOH NS vs EtOH + TMT $t_{21.66}$=3.67, ##p=0.0082. **K**, oEPSC normalized amplitude across 10 Hz pulse trains: pulse main effect $F_{9,342}$=69.96, p<0.0001; Pulse

7: H_2O vs EtOH + TMT $t_{19.59}$=2.94, ^p=0.0498; Pulse 10: H_2O vs EtOH + TMT $t_{18.14}$=3.05, ^p=0.0410.

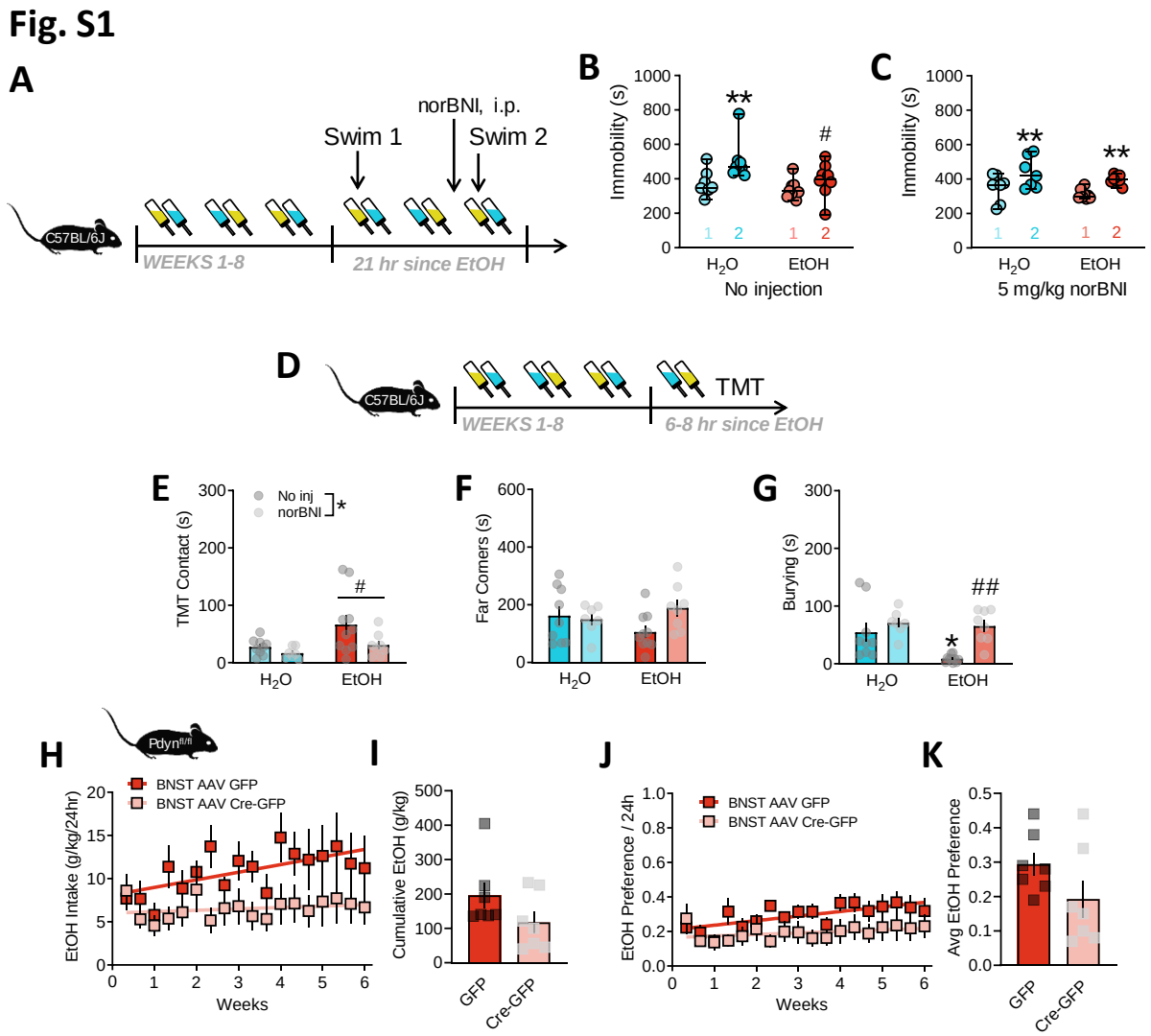

Fig. S1. A, Design of testing repeated forced swim behavior during acute withdrawal from EtOH (n=9) or H_2O controls (n=8). **B**, Immobility time (sec) during first (light aqua, light red) and second (aqua, red) forced swim tests in H_2O and EtOH mice. Main effect of Swim trial $F_{1,15}$=19.70, p=0.0005; H_2O Swim 1 vs Swim 2 t_{15}=4.29, **p=0.0013; Swim 2 H_2O vs EtOH t_{30}=2.63, #p=0.0266. **C**, Immobility time (sec) after 5 mg/kg norBNI injection before the second swim test in EtOH (n=8) and H_2O mice (n=7). Main effect of Swim trial $F_{1,13}$=36.60, p<0.0001; H_2O Swim 1 vs Swim 2 t_{13}=4.17, **p=0.0022; EtOH Swim 1 vs Swim 2 t_{13}=4.40, **p=0.0014. **D**, Schematic of TMT predator odor testing during acute withdrawal from EtOH (n=10) or H_2O controls (n=10) and norBNI-treated EtOH (n=7) and H_2O mice (n=8). **E**, TMT contact (sec): EtOH main effect $F_{1,30}$=4.26, #p=0.0479; norBNI main effect $F_{1,30}$=5.53, *p=0.0255. **F**, Far corners (sec). **G**, Burying (sec): EtOH main effect $F_{1,30}$=12.06, p=0.0016; H_2O no injection vs EtOH no injection t_{30}=3.28, *p=0.0156. NorBNI main effect $F_{1,30}$=5.95, p=0.0208. EtOH no injection vs norBNI t_{30}=3.93, ##p=0.0028. **H**, *Pdyn*$^{lox/lox}$ mice EtOH drinking (g/kg/24hr) across 6 wks with BNST GFP (red) or Cre-GFP (light red): interaction $F_{17,204}$=1.49, p=0.1003. **I**, Cumulative EtOH drinking (g/kg) per group: t_{12}=1.63, p=0.1299. **J**, *Pdyn*$^{lox/lox}$ mice daily EtOH preference across 6 wks with BNST GFP (red) or Cre-GFP (light red): Time main effect $F_{17,204}$=2.74, p=0.0256. **K**, Average EtOH preference per group: t_{12}=1.61, p=0.1340.

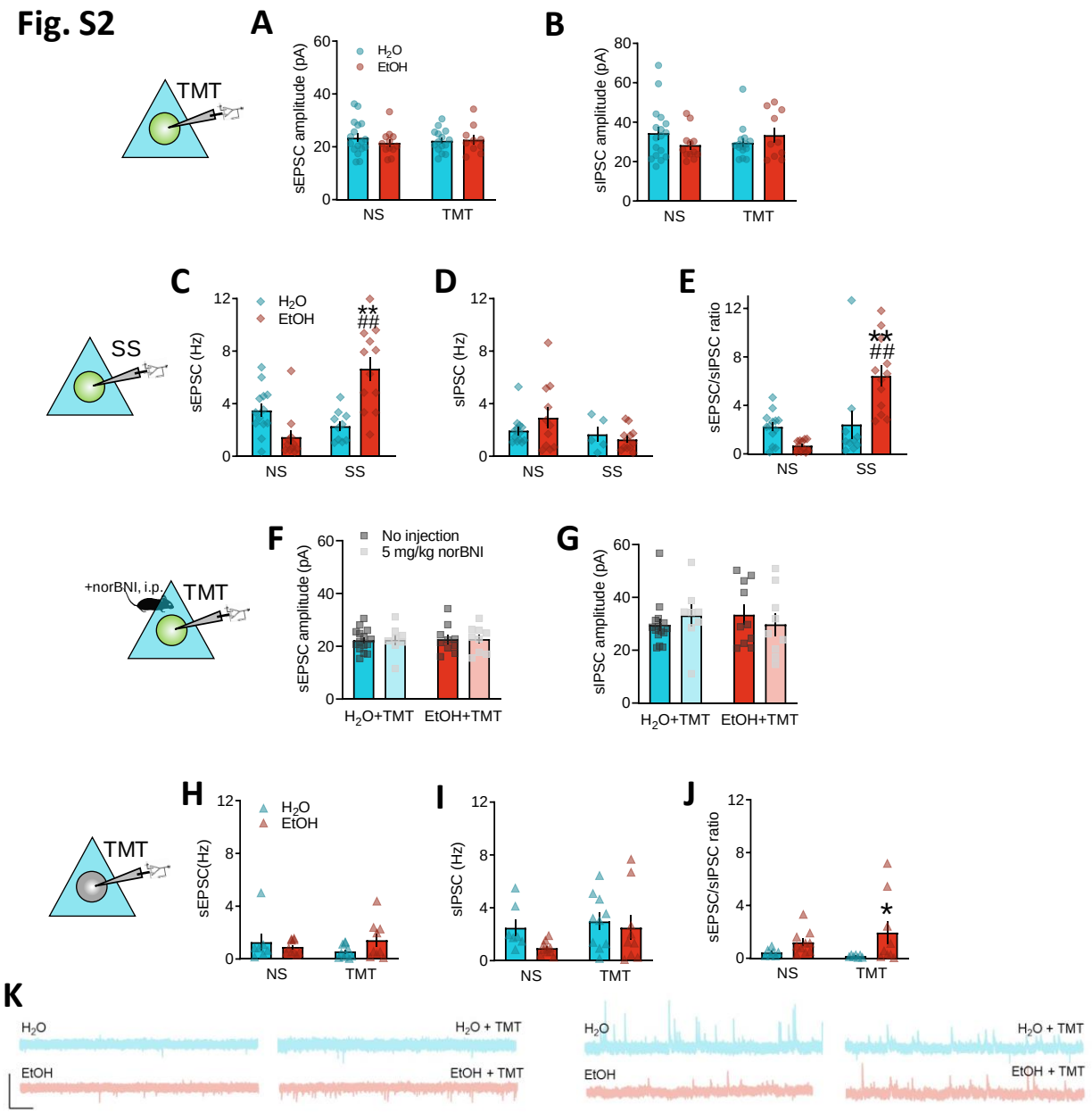

Fig. S2. A, TMT BNST^{PDYN} cell synaptic transmission sEPSC amplitude (pA). **B**, sIPSC amplitude (pA). **C**, Swim stress (SS) BNST^{PDYN} cell sEPSC frequency (Hz; H_2O n=4, 13 cells; EtOH n=3, 11 cells; H_2O + SS n=3, 10 cells; EtOH + SS n=4, 12 cells): interaction $F_{1,42}$=26.07, p<0.001; H_2O + SS vs EtOH + SS t_{42}=4.82, **p=0.0001; EtOH NS vs SS t_{42}=5.89, ##p<0.0001. **D**, sIPSC frequency (Hz). **E**, sEPSC/sIPSC ratio: interaction $F_{1,42}$=14.79, p=0.0004; H_2O + SS vs EtOH + SS t_{42}=3.84, **p=0.0004; EtOH NS vs SS t_{42}=5.65, ##p<0.0001. **F**, NorBNI pretreatment BNST^{PDYN} cell sEPSC amplitude (pA). **G**, sIPSC amplitude (pA). **H**, BNST non-GFP-labeled cell synaptic transmission sEPSC frequency (Hz; H_2O n=3, 7 cells; EtOH n=3, 10 cells; H_2O + TMT n=3, 10 cells; EtOH + TMT n=3, 9 cells). **I**, sIPSC frequency (Hz). **J**, sEPSC/sIPSC ratio: EtOH main effect $F_{1,32}$=7.12, p=0.0119; TMT H_2O vs TMT EtOH t_{32}=2.70, *p=0.0216. **K**, Representative traces of BNST non-GFP cells. Scale bar indicates 50 pA height and 1 sec time.

Fig. S3

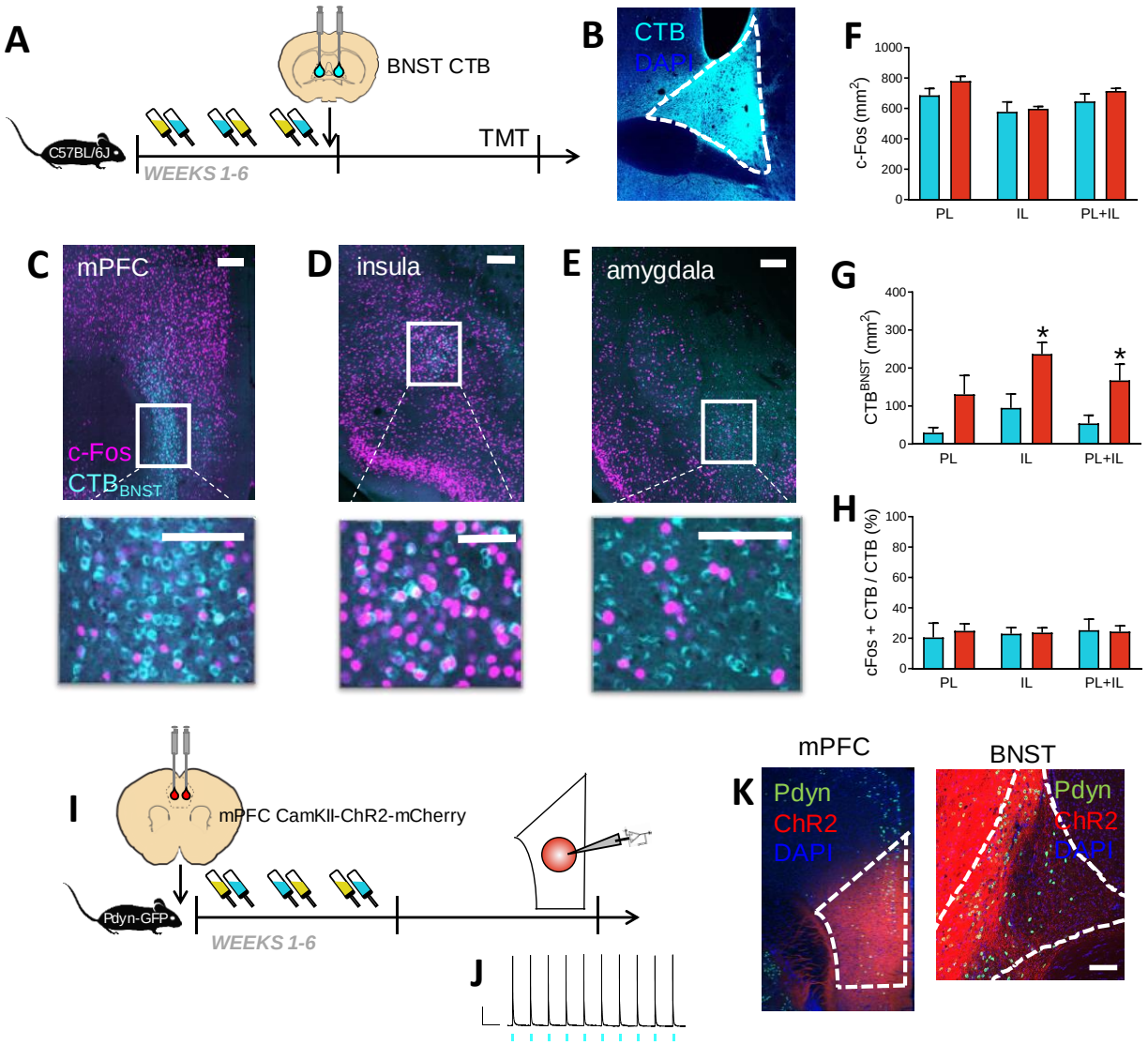

Fig. S3. A, Schematic of choleratoxin B (CTB) retrograde tracing in BNST before TMT and c-Fos immunohistochemistry. **B**, Image of CTB injection into the BNST. c-Fos immunostaining (pseudocolored purple) and CTB 555 from the BNST (pseudocolored aqua) in the **C**, medial prefrontal cortex (mPFC), **D**, insula, **E**, amygdala. Scale bars measure 200 µm. Inset photo scale bars measure 100 µm. **F**, mPFC c-Fos quantification (mm^2) in prelimbic (PL), infralimbic (IL), and combined PL+IL. Aqua bars are H_2O (n=3), red bars are EtOH (n=4). **G**, CTB quantification from the BNST: IL H_2O vs EtOH t_5=2.82, *p=0.0369; PL+IL H_2O vs EtOH t_5=2.58, *p=.0496. **H**, Percentage of colocalization of c-Fos and CTB over total CTB (%). **I**, Design of synaptic strength physiology experiments from mPFC to BNST^{PDYN} cells. **J**, Representative traces of optically-evoked mPFC action potentials at 1 Hz. Blue rectangles indicate 470nm LED onset. Scale bar indicates 20 mV and 1 sec. **K**, Image of CamKII-ChR2-mCherry expression in the mPFC (left) and at BNST terminals (right). Pdyn-GFP cells are green. Inset photo scale bars measure 100 µm.